Received: 12 January 2019 | Revised: 18 March 2019 | Accepted: 19 March 2019

DOI: 10.1002/aoc.4945

WILEY Applied Organometallic Chemistry

FULL PAPER

Inner metal complexes of tetradentate Schiff base: Synthesis, characterization, biological activity and molecular docking studies

M.A. Diab[1] | Gehad G. Mohamed[2,3] | W.H. Mahmoud[2] | A.Z. El-Sonbati[1] | Sh.M. Morgan[4] | S.Y. Abbas[1]

[1]Chemistry Department, Faculty of Science, Damietta University, Egypt

[2]Chemistry Department, Faculty of Science, Cairo University, Giza 12613, Egypt

[3]Egypt Nanotechnology Center, Cairo University, El-Sheikh Zayed, 6th October, 12588, Egypt

[4]Environmental Monitoring Laboratories, Ministry of Health, Port Said, Egypt

Correspondence
Gehad G. Mohamed, Chemistry Department, Faculty of Science, Cairo University, Giza 12613, Egypt.
Email: ggenidymohamed@sci.cu.edu.eg

A novel Schiff base ligand, namely 2,2′-((1*E*,1′*E*)-(1,3-phenylenebis(azanylylidene))bis(methanylylidene))diphenol (H_2L), was synthesized by condensation of *m*-phenylenediamine and 2-hydroxybenzaldehyde (in 1:2 ratio). Series of complexes were obtained from the reaction of La(III), Er(III) and Yb(III) chlorides with H_2L. The ligand and complexes were characterized using elemental analysis, infrared, ^{1}H NMR, UV–visible and mass spectroscopies, magnetic susceptibility and conductivity measurements and thermal analysis. Infrared and ^{1}H NMR spectra indicated the coordination of the azomethine nitrogens and deprotonated phenolic oxygen atoms in a tetradentate manner (ONNO). The thermal behaviour of the complexes was studied from ambient temperature to 1000°C. The complexes were found to have water molecules of hydration and coordinated water molecules. The complexes were found to possess high biological activities against various organisms compared to the free ligand (Gram-positive bacteria *Staphylococcus aureus* and *Bacillus subtilis*, Gram-negative bacteria *Salmonella* sp., *Escherichia coli* and *Pseudomonas aeruginosa* and fungi *Aspergillus fumigatus* and *Candida albicans*). The more effective and probable binding modes between H_2L with different active sites of colon cancer (PDB code: 2hq6) and lung cancer (PDB code: 1x2j) receptors were investigated using molecular docking studies.

KEYWORDS
biological activity, molecular docking, Schiff base metal(III) complexes, spectroscopic analyses, thermal analysis

1 | INTRODUCTION

Schiff bases are unique compounds due to the possibility of easily varying fragments at the exocyclic C=N bond, which allows exploring such important aspects as tautomerism, conformational equilibria, acid–base and donor–acceptor properties, etc. But, probably, the most important property of azomethines is their high complex-forming ability.[1,2] The formation of macrocyclic complexes depends significantly on the dimension of internal cavities, the rigidity of the macrocycles, the nature of its donor atoms and the complexing properties of the anion involved in the coordination.[3,4] The interest in azomethines and their metal complexes is due to the application of these complexes as metalloenzymes[5,6] and in hosting and carrying small molecules[7] or

catalysis.[8] Among them are luminophores, lubricants, fuel additives, photochromic materials, biologically active compounds, etc.[9] Due to the superior properties of Schiff base–metal complexes, interactions of these complexes with proteins such as DNA and albumins have been extensively studied.[10] For decades, the coordination chemistry of Schiff base ligands has been the subject of great interest. Schiff bases are capable of forming coordinate bonds with many metal ions via azomethine, phenolic or thiolic groups, and so they have been used for the synthesis of metal complexes due to their easy formation and strong metal binding ability. During recent years, coordination compounds of biologically active ligands[11,12] have received much attention. Chelation causes marked change in the biological properties of ligands and also the metal moieties. It has been reported that chelation is the cause and cure of many diseases including cancer. Binding studies of transition metal complexes with DNA have had a vital role in the development of DNA molecule probes and chemotherapeutics in recent years.[13] In order to find anticarcinogens that can recognize and cleave DNA, many kinds of complexes have been synthesized and developed. Among these complexes, metals or ligands can be varied in an easily controlled way to facilitate individual applications.[14] Therefore, current research involving metal complexes of Schiff bases has expanded enormously and embraces diversified subjects comprising their various aspects in bio-coordination and bio-inorganic chemistry.

In our ongoing research, a novel Schiff base ligand, namely 2,2′-((1*E*,1′*E*)-(1,3-phenylenebis(azanylylidene)) bis(methanylylidene))diphenol (H_2L), was synthesized. Complexes were synthesized from the reaction of H_2L with La(III), Er(III) and Yb(III) chlorides and characterized using elemental analysis, spectroscopic techniques, conductivity and magnetic susceptibility measurements and thermal analysis. The new compounds were investigated for their antimicrobial and antifungal activities against various organisms and compared with those of standard antibacterial and antifungal drugs. The calculated binding energy values of the receptors of the structure of colon cancer (PDB code: 2hq6) and lung cancer (PDB code: 1x2j) were determined.

2 | EXPERIMENTAL

2.1 | Materials and reagents

All chemicals used were of analytical reagent grade (AR) and of the highest purity available. They included 2-hydroxybenzaldehyde (Merck), *m*-phenylenediamine (Merck), $LaCl_3{\cdot}7H_2O$, $ErCl_3{\cdot}6H_2O$ and $YbCl_3{\cdot}6H_2O$ (Sigma-Aldrich). The organic solvents such as absolute ethyl alcohol and dimethylformamide (DMF) were spectroscopically pure from BDH.

2.2 | Instrumentation

Microanalyses of carbon, hydrogen and nitrogen were carried out at the Microanalytical Centre, Cairo University, Egypt, using a CHNS-932 (LECO) Vario elemental analyser. Fourier transform infrared (FT-IR) spectra were recorded with a PerkinElmer 1650 spectrometer (400–4000 cm^{-1}) using KBr pellets. Electronic spectra were recorded at room temperature with a Shimadzu 3101pc spectrophotometer as solutions in DMF. Mass spectra were recorded using the EI technique at 70 eV with a Hewlett-Packard MS-5988 GS-MS instrument at the Microanalytical Centre, National Centre for Research, Egypt. Molar magnetic susceptibility was measured with powdered samples using the Faraday method. Diamagnetic corrections were made with Pascal's constant and $Hg[Co(SCN)_4]$ was used as a calibrant. Molar conductivities of 10^{-3} M solutions of the complexes in DMF were measured using a Jenway 4010 conductivity meter. Thermogravimetric analysis (TGA) of the solid complexes was carried out from room temperature to 1000 °C using a Shimadzu TG-50H thermal analyser. The antimicrobial activities were determined at the Microanalytical Centre, Cairo University, Egypt. The UV–visible electronic spectra of 1×10^{-4} M solutions of H_2L and its metal complexes prepared by accurate dilution from previously prepared stock solutions were obtained in the wavelength range from 200 to 700 nm. Docking calculations were carried out on receptors of the structure of the cyclophilin_CeCYP16-like domain of the serologically defined colon cancer Antigen 10 from *Homo sapiens* (PDB code: 2hq6) and the structural basis for the defects of human lung cancer somatic mutations in the repression activity of Keap1 on Nrf2 (PDB code: 1x2j). The MMFF94 force field was used for energy minimization of molecules using Docking Server.[15–19]

2.3 | Synthesis of Schiff base ligand H_2L

The new Schiff base ligand was synthesized by the condensation reaction of *m*-phenylenediamine with 2-hydroxybenzaldehyde. A solution of 2-hydroxyben zaldehyde (74 mmol, 9.04 g, 7.74 mL) dissolved in ethanol was added dropwise to *m*-phenylenediamine (37 mmol, 4 g) dissolved in ethanol. The resulting mixture was stirred under reflux for about 3 h at 100–150 °C during which an orange solid compound was separated. It was filtered, recrystallized, washed several times with ethanol

and with diethyl ether and dried in vacuum (Scheme 1). Yield 52.33%; m.p. 115 °C; green solid. Anal. calcd for $C_{20}H_{16}N_2O_2$ (%): C, 75.95; H, 5.06; N, 8.86. Found (%): C, 75.93; H, 5.05; N, 8.85. FT-IR (cm^{-1}): phenolic ν(OH) 3438, azomethine ν(C=N) 1617, ν(C—N) 1386, ν(C—O) phenolic 1276. ^{1}H NMR (300 MHz, DMSO-d_6, δ, ppm): 13.00 (s, 2H, OH phenolic), 9.05 (s, 2H, CH=N), 6.91–8.71 (m, 12H, ArH). λ_{max} (cm^{-1}): 36 496 π–π*, 28 985 n–π*.

2.4 | Synthesis of metal complexes of H_2L

The metal complexes were prepared by the addition of a hot solution (60 °C) of the appropriate metal chloride (1.266 mmol) in ethanol to a hot solution (60 °C) of the ligand (0.4 g, 1.266 mmol) in a mixture of ethanol and DMF in a ratio of 2:1 (v/v). The resulting mixture was stirred under reflux for 2 h, whereupon the complexes precipitated. They were removed by filtration and purified by washing several times with hot ethanol and diethyl ether. The analytical data for C, H and N were determined in duplicate.

2.4.1 | $[La(L)(H_2O)_2]\cdot Cl\cdot H_2O$ (1)

Yield 36.44%; dark brown solid, m.p. 127 °C. Anal. calcd for $La(C_{20}H_{20}ClN_2O_5)$ (%): C, 44.25; H, 3.69; N, 5.16; La, 25.61. Found (%): C, 44.23; H, 3.71; N, 5.17; La, 25.60. FT-IR (cm^{-1}): azomethine ν(C=N) 1654, ν(C—N) 1384, phenolic ν(C—O) 1248, ν(H_2O) stretching bands of coordinated water 964 and 858, ν(M—O) stretching bands of coordinated water 580, metal–oxygen bond ν(M—O) 591, metal–nitrogen bond ν(M—N) 430. Molar conductivity (10^{-3} M, DMF): 98.60 Ω^{-1} cm^2 mol^{-1}. μ_{eff} = 5.46 BM. λ_{max} (cm^{-1}): 36,630 π–π*, 31,948 n–π*.

2.4.2 | $[Er(L)(H_2O)_2]\cdot Cl\cdot H_2O$ (2)

Yield 34.63%; dark brown solid, m.p. 232 °C. Anal. calcd for $Er(C_{20}H_{20}ClN_2O_5)$ (%): C, 42.05; H, 3.51; N, 4.91; Er, 29.31. Found (%): C, 42.02; H, 3.50; N, 4.92; Er, 29.33. FT-IR (cm^{-1}): azomethine ν(C=N) 1651, ν(C—N) 1384, phenolic ν(C—O) 1248, ν(H_2O) stretching bands of coordinated water 960 and 851, ν(M—O) stretching bands of coordinated water 577, metal–oxygen bond ν(M—O) 585, metal–nitrogen bond ν(M—N) 476. Molar conductivity (10^{-3} M, DMF): 91.50 Ω^{-1} cm^2 mol^{-1}. μ_{eff} = 5.46 BM. λ_{max} (cm^{-1}): 36 496 π–π*.

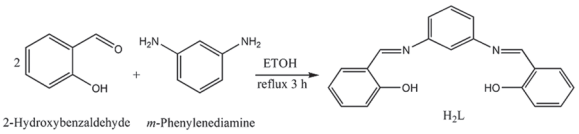

SCHEME 1 Preparation of Schiff base ligand (H_2L)

2.4.3 | $[Yb(L)(H_2O)_2]\cdot Cl\cdot H_2O$ (3)

Yield 41.14%; dark brown solid, m.p. 257 °C. Anal. calcd for $Yb(C_{20}H_{20}ClN_2O_5)$ (%): C, 41.63; H, 3.47; N, 4.86; Yb, 30.02. Found (%): C, 41.60; H, 3.48; N, 4.87; Yb, 30.01. FT-IR (cm^{-1}): azomethine ν(C=N) 1656, ν(C—N) 1384, phenolic ν(C—O) 1244, ν(H_2O) stretching bands of coordinated water 914 and 854, ν(M—O) stretching bands of coordinated water 529, metal–oxygen bond ν(M—O) 538, metal–nitrogen bond ν(M—N) 456. Molar conductivity (10^{-3} M, DMF): 90.90 Ω^{-1} cm^2 mol^{-1}. μ_{eff} = 5.46 BM. λ_{max} (cm^{-1}): 36 496 π–π*.

2.5 | Biological activity

The antimicrobial activity of the complexes was determined using a modified Kirby–Bauer disc diffusion method.[2,20] An amount of 100 μl of the test bacteria or fungi was added to 10 ml of fresh media until cultures reached a count of approximately 10^8 cells ml^{-1} for bacteria and 10^5 cells ml^{-1} for fungi.[21] An amount of 100 μl of microbial suspension was spread onto agar plates corresponding to the broth in which they were maintained. Isolated colonies of each organism that might play a pathogenic role were selected from primary agar plates and tested for susceptibility by the disc diffusion method. Of the many media available, NCCLS recommends Mueller-Hinton agar due to it resulting in good batch-to-batch reproducibility. The disc diffusion method for filamentous fungi tested using an approved standard method (M38-A) was developed[22] for evaluating the susceptibilities of filamentous fungi to antifungal agents. The disc diffusion method for yeast was developed using approved standard method (M44-P).[23]

Plates inoculated with Gram-positive bacteria *Staphylococcus aureus* and *Bacillus subtilis* and Gram-negative bacteria *Pseudomonas aeruginosa*, *Salmonella* sp. and *Escherichia coli* were incubated at 35–37 °C for 24–28 h. Fungi *Aspergillus fumigatus* and *Candida albicans* were incubated at 30 °C for 24–28 h. Then the diameters of the inhibition zones were measured in millimeters.[23] Standard discs of ampicillin and gentamycin (antibacterial agents) and amphotericin B (antifungal agent) served as positive controls for antimicrobial activity. Filter discs impregnated with 10 μl of solvent (distilled water, chloroform, dimethylsulfoxide (DMSO)) were used as a negative control. The agar used was Mueller-Hinton agar that is rigorously tested for composition

and pH. Further, the depth of the agar in the plate is a factor to be considered in the disc diffusion method. This method is well documented and standard zones of inhibition have been determined for susceptible and resistant values. Blank paper discs (Schleicher and Schuell, Spain) with a diameter of 8.0 mm were impregnated with 10 μl of test concentrations of stock solutions. When a filter paper disc impregnated with a test chemical is placed on agar, the chemical will diffuse from the disc into the agar. This diffusion will place the chemical in the agar only around the disc. The solubility of the chemical and its molecular size will determine the size of the area of chemical infiltration around the disc. If an organism is placed on the agar, it will not grow in the area around the disc if it is susceptible to the chemical. This area of no growth around the disc is known as zone of inhibition or clear zone. For the disc diffusion method, the zone diameters were measured with slipping calipers of the National Committee for Clinical Laboratory Standards.[24] Agar-based methods such Etest and disc diffusion can be good alternatives because they are simpler and faster than broth-based methods.[25]

3 | RESULTS AND DISCUSSION

3.1 | Characterization of Schiff base ligand

The symmetric Schiff base ligand was prepared by stirring an appropriate amount of 2-hydroxybenzaldehyde with the corresponding *m*-phenylenediamine (2:1) in ethanol. The new Schiff base ligand formed was characterized with respect to its composition using elemental and spectral analyses.

3.1.1 | Elemental analysis

The synthesized Schiff base ligand H_2L is stable at room temperature. The elemental analysis results (C, H, and N) are in good agreement with those calculated for the suggested formula presented in section 2. The melting point is sharp indicating the purity of the prepared ligand. The ligand is found to be soluble in DMF and DMSO.

3.1.2 | Mass spectromtric study

The electron impact spectrum of the newly prepared Schiff base ligand was recorded and investigated at an electron energy of 70 eV. It is obvious that the molecular ion peaks are in good agreement with its suggested empirical formula as indicated from elemental analyses. The mass spectrum of the ligand shows a peak at $m/z = 316$ (M^+) which refers to the main molecular ion of the Schiff base (molar mass = 316 g mol^{-1}).

3.1.3 | FT-IR spectrum

The FT-IR spectrum of the free ligand is characterized mainly by the strong bands at 3438, 1386 and 1276 cm^{-1}, corresponding to the stretching frequencies of ν(OH) phenolic, ν(C—N) stretching and ν(C—O) phenolic, respectively. Also a band at 1617 cm^{-1} for the azomethine ν(C=N) stretching vibration was recorded due to the condensation reaction between *m*-phenylenediamine and 2-hydroxybenzaldehyde, confirming the formation of the Schiff base ligand.[26]

3.1.4 | ^{1}H NMR spectral study

The ^{1}H NMR spectrum of the newly synthesized Schiff base ligand features peaks appearing at 6.91–8.71 ppm (m, 12H) which may be assigned to the aromatic ring protons. A sharp band at 9.05 ppm (s, 2H) may be assigned to the protons of azomethine (—CH=N—) groups which confirms the formation of the Schiff base ligand.[27,28] A singlet peak at 13.00 ppm (s, 2H, OH) can be assigned to the protons of OH phenolic groups.[29] A peak at 4.23 ppm is attributed to the protons of amine NH_2 group. It is observed from ^{1}H NMR data that the aldehyde and amine protons completely disappeared with the formation of a new azomethine bond.

3.2 | Molecular docking study of Schiff base ligand

The purpose of studying molecular docking is to simulate the molecular recognition process by achieving an optimized conformation for a protein and a drug with relative orientation between them such that the free energy of the overall system is minimized.[30–35] Exploration of the molecular docking interaction of H_2L was performed using Docking Server.[30,31] Affinity of molecules to anticancer receptors is very important in drug design. Therefore, we carried out molecular docking of H_2L with different anticancer protein targets, namely colon cancer (PDB code: 2hq6) and lung cancer (PDB code: 1x2j). H_2L was evaluated for its inhibitory effect on receptors of 2hq6 and 1x2j. The data showed a favourable arrangement between H_2L and the receptors and the interaction curves are shown in Figure 1. The calculated energy as well as some parameters

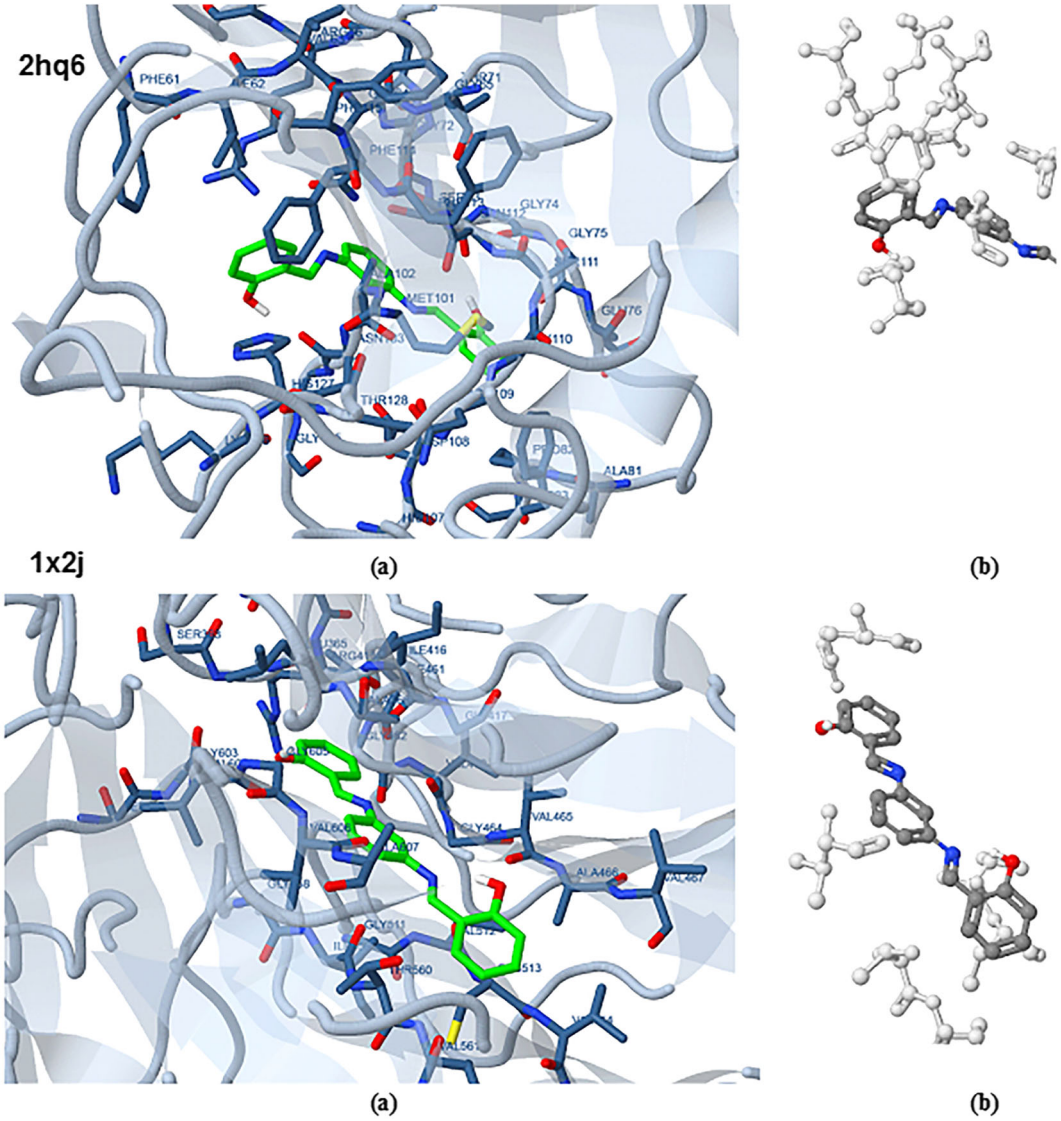

FIGURE 1 The Schiff base ligand (H_2L) (green in (a) and grey in (b)) in interaction with receptors of colon cancer (PDB code: 2hq6) and lung cancer (PDB code: 1x2j)

concerning the selected anticancer receptors are listed in Table 1. A more negative charge represents a more stable interaction. The two-dimensional plots of binding for H_2L with the receptors of 2hq6 and 1x2j are shown in Figure 2, showing binding interaction sites of H_2L with protein active sites of 2hq6 and 1x2j. The HB plots explain the interactions between H_2L and receptors of 2hq6 and 1x2j as shown in Figures 3 and 4. Some parameters were estimated using AutoDock and are presented in Table 1. Estimated free energy of binding, estimated inhibition constant (K_i) and interaction surface area reveal the most favoured binding. The more negative value of estimated free energy of binding represents more efficient binding. And therefore, the order of best

TABLE 1 Energy values and parameters obtained in docking calculations for H_2L with receptors of colon cancer (PDB code: 2hq6) and lung cancer (PDB code: 1x2j)

Receptor	Estimated free energy of binding (kcal mol^{-1})	Estimated inhibition constant, K_i (μM)	vdW + bond + desolv energy (kcal mol^{-1})	Electrostatic energy (kcal mol^{-1})	Total intercooled energy (kcal mol^{-1})	Interaction surface (Å)
2hq6	−6.28	24.72	−8.04	−0.16	−8.19	786.279
1x2j	−7.69	2.33	−8.97	−0.10	−9.06	832.183

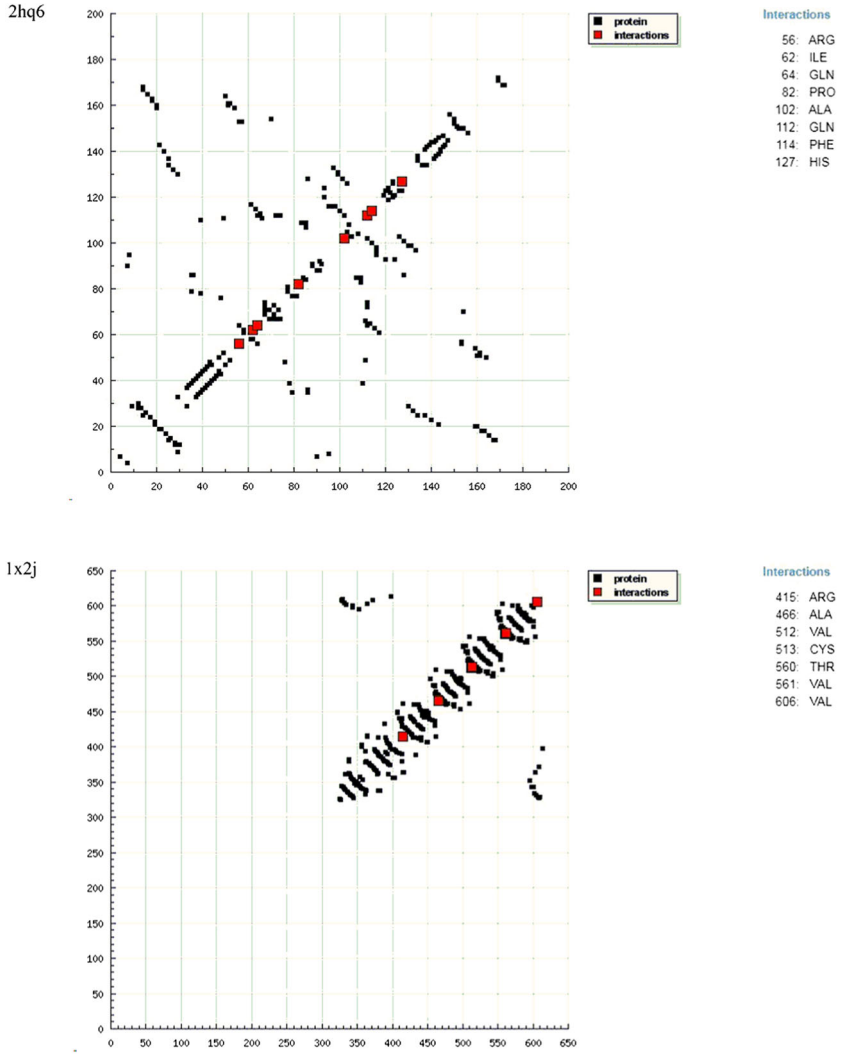

FIGURE 2 HB plot of interaction between Schiff base ligand (H_2L) and receptors of colon cancer (PDB code: 2hq6) and lung cancer (PDB code: 1x2j)

binding of the selected target anticancer receptors towards H_2L is found to be: 1x2j > 2hq6. So the interaction between H_2L and anticancer receptors means its use for cancer treatment is possible.

3.3 | Compositions and structures of metal complexes

3.3.1 | Elemental analyses and magnetic susceptibility measurement

The solid complexes were prepared by mixing a hot solution of H_2L with aqueous solutions of La(III), Er(III) and Yb(III) salts forming immediate precipitates of the metal complexes. All the synthesized complexes are quite air stable, non-hygroscopic and insoluble in water but readily soluble in DMF. The elemental and spectral analyses of the complexes suggested that their composition was 1:1 metal-to-ligand stoichiometries and agreed with the formula of [ML] type for all complexes. The magnetic susceptibility values suggest an octahedral geometry of the synthesized complexes.

3.3.2 | Molar conductance measurements

Molar conductivities of the complexes were measured with 10^{-3} M concentrations in DMF solution as a solvent at room temperature and the results are presented in section 2. Generally, higher molar conductance values are indicative of the electrolytic nature of metal complexes and lower values show a non-electrolytic nature. Molar conductivity values of La(III), Er(III) and Yb(III) complexes are equal to 98.60, 91.50 and 90.90 Ω^{-1} cm^2 mol^{-1}, respectively, indicating the electrolytic behaviour (1:1) of these complexes.

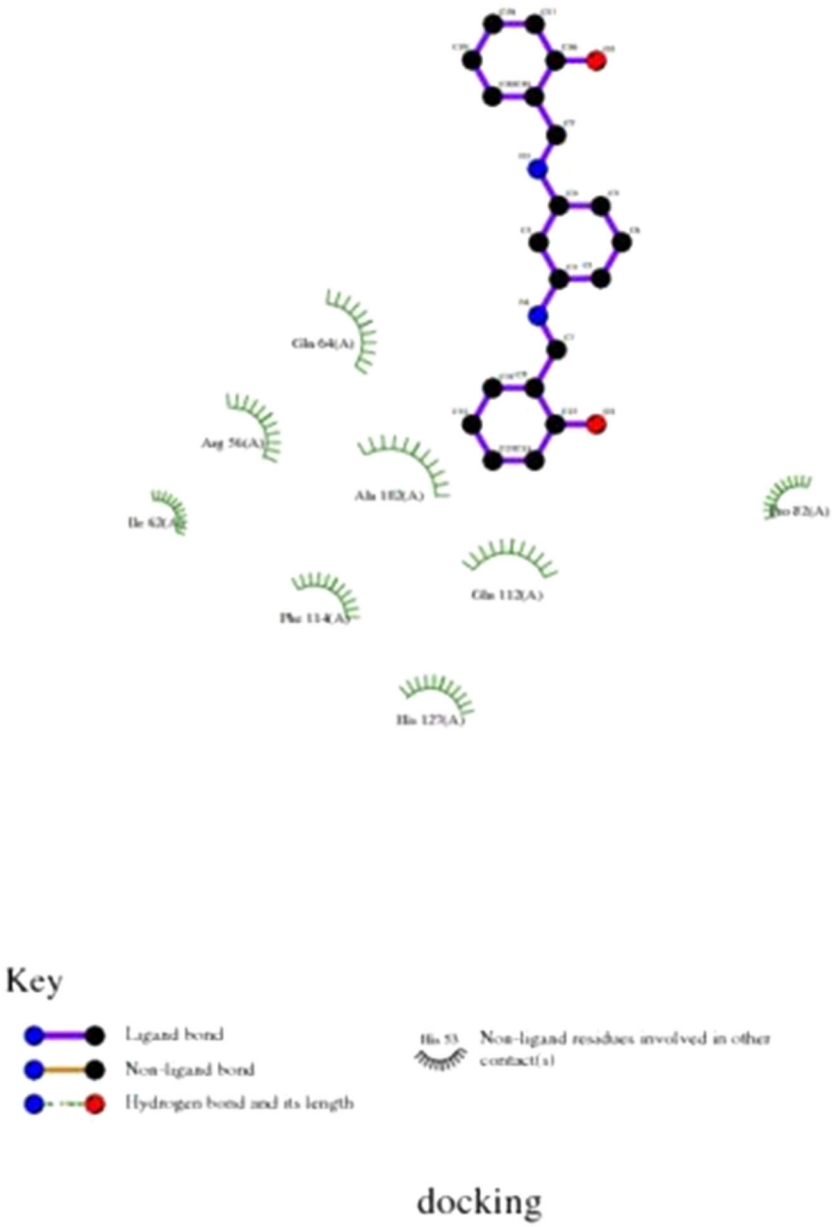

FIGURE 3 Two-dimensional plot of interaction between Schiff base ligand (H_2L) and receptors of colon cancer (PDB code: 2hq6)

3.3.3 | FT-IR spectra

The important FT-IR spectral bands and their assignments are discussed here. The ν(C—O) stretching for the free ligand at 1276 cm^{-1} is shifted to lower frequencies for all the metal complexes, giving strong absorption bands at *ca* 1248, 1248 and 1248 cm^{-1} for La(III), Er(III) and Yb(III) complexes, respectively. This clearly indicates the coordination of oxygen of phenolic groups in these complexes with proton displacement. The broad band at *ca* 3438 cm^{-1} observed for the ligand was found at *ca* 3406–3416 cm^{-1} fort the complexes, which was attributed to ν(OH) of coordinated and hydrated water molecules. In the investigated metal complexes, the bands observed in the regions 3406–3416, 914–964 and 858–851 cm^{-1} are attributed to —OH stretching, bonding, rocking and wagging vibrations, due to the presence of water molecules. The presence of rocking band indicates the coordination nature of water molecules.[36–39] The FT-IR spectrum of the ligand shows a strong band at *ca* 1617 cm^{-1} which is attributed to ν(HC=N). The shift of this peak for the complexes to higher frequency in the range 1651–1656 cm^{-1} is an indication of the coordination of the nitrogen atom of HC=N group to the metal ion in the complexes.[2,9,36] As expected, for the complexes, this is observed due to possible donation of the lone pair electron density towards the metal ion and makes strong evidence for the coordination of HC=N through nitrogen to the metal ions. New peaks observed for the metal complexes at 430–476 and 529–580 cm^{-1}, assigned to M—N and M—O, respectively, provide additional confirmation for coordination of the oxygen atom

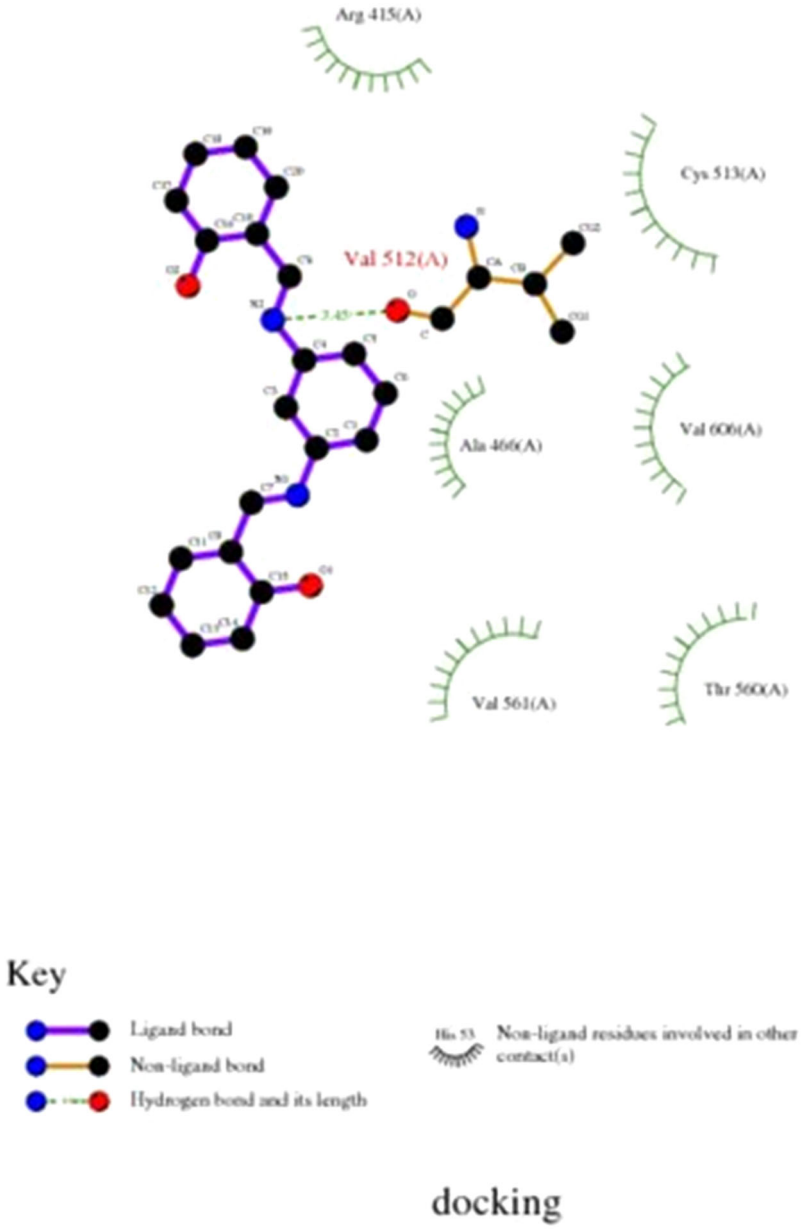

FIGURE 4 Two-dimensional plot of interaction between Schiff base ligand (H_2L) and receptors of lung cancer (PDB code: 1x2j)

of phenolic group and the imino group of the ligand with the metal ions.[40–42] The ν(M—O) stretching vibrations of coordinated water attached to metal ions are found at 529–580 cm^{-1} for the complexes.[2,20,40] The FT-IR spectral data of ligand and its metal complexes are summarized in Table 2.

It is concluded from the FT-IR spectral data that the Schiff base is a binegative tetradentate ligand coordinated to the metal ions through two deprotonated phenolic oxygen atoms and two azomethine nitrogen atoms.

3.3.4 | Mass spectra

The mass spectrum of the La(III) complex showed a prominent peak at m/z = 542 (M^+), equivalent to its molecular weight and confirming the molecular formula $[La(L)(H_2O)_2]Cl{\cdot}H_2O$. The structure of the complex was confirmed by the presence of a peak at m/z = 316 corresponding to the ligand moiety ($C_{20}H_{16}N_2O_2$, atomic mass of 316 amu).

3.4 | Thermal analyses

The thermal decomposition process of H_2L with the molecular formula $[C_{20}H_{16}N_2O_2]$ involves four decomposition steps (Table 3). The first stage of decomposition involves the loss of $C_4H_6O_2$ molecule at 45–305 °C, and is accompanied by a weight loss of *ca* 27.21% (calcd 27.22%). The second stage of decomposition occurs in the range 305–535 °C, corresponding to the loss of

TABLE 2 FT-IR spectral data of H_2L and its metal complexes[a]

H_2L	1	2	3	Assignment
3438b	3406	3416	3416	OH stretching
1617	1654	1651	1656	CH=N stretching
1386	1384	1384	1384	C—N stretching
1276	1248	1248	1244	C—O phenolic
—	964, 858s	960, 851s	914, 854s	H_2O stretch of coordinated water
—	591w	585s	538s	M—O
—	580s	577s	529s	M—O stretching of coordinated water
—	430w	476s	456s	M—N

[a]Numbers are given in section 2.

TABLE 3 TGA data of H_2L and its metal complexes[a]

Complex	TGA range (°C)	DTG_{max} (°C)	*n**	Mass loss; total mass loss Estimated (calcd) (%)	Assignment	Residues
H_2L	45–305	225	1	27.21 (27.22)	- Loss of $C_4H_6O_2$	—
	305–535	409	1	25.30 (25.31)	- Loss of $C_4H_4N_2$	
	535–700	619	1	24.03 (24.05)	- Loss of C_6H_4	
	700–1000	782	1	23.41 (23.42); 99.95 (100)	- Loss of C_6H_2	
$[La(L)(H_2O)_2]Cl{\cdot}H_2O$	30–115	82	1	16.14 (16.68)	- Loss of $3H_2O$ and HCl	$½La_2O_3$ + 4C
	115–375	258	1	18.05 (18.07)	- Loss of $C_6NH_4O_{0.5}$	
	375–655	460	1	10.12 (10.14)	- Loss of C_3NH_5	
	655–1000	775	1	16.21 (16.23); 60.52 (61.12)	- Loss of C_7H_4	
$[Er(L)(H_2O)_2]Cl{\cdot}H_2O$	30–150	80	1	16.02 (16.12)	- Loss of $3H_2O$, HCl and H_2	$½Er_2O_3$ + 11C
	150–415	257	1	13.97 (14.02)	- Loss of $C_4N_2H_4$	
	415–1000	936	1	13.12 (13.14); 43.11 (43.28)	- Loss of C_4H_6 and $½C_2H_2O$	
$[Yb(L)(H_2O)_2]Cl{\cdot}H_2O$	30–100	77	1	14.47 (14.48)	- Loss of $2.5H_2O$, H_2 and HCl	$½Yb_2O_3$ + 6C
	100–340	210	1	17.64 (17.69)	- Loss of $C_4H_{10}N_2O$	
	340–1000	530	1	20.98 (21.16); 53.09 (53.33)	- Loss of $C_{10}H_2$	

[a]Numbers are given in section 2.

$C_4H_4N_2$ molecule, and is accompanied by a weight loss of *ca* 25.30% (calcd 25.31%). The third stage involves the removal of C_6H_4 molecule in the range 535–700 °C, and is accompanied by a weight loss of *ca* 24.03% (calcd 24.05%). The fourth stage involves the removal of C_6H_2 molecule in the range 700–1000 °C, and is accompanied by a weight loss of *ca* 23.41% (calcd 23.42%). The total weight loss amounts to 99.95% (calcd 100%).

The TGA plot of **1** displayed four decomposition steps. The first step occurred in the range 30–115 °C with a weight loss of *ca* 16.14% (calcd 16.68%) due to the release of three molecules of H_2O and one of HCl.[40–42] The second step occurred in the range 115–375 °C with a weight loss of *ca* 18.05% (calcd 18.07%) attributed to the loss of $C_6NH_4O_{0.5}$ molecule. The third step occurred in the range 375–655 °C with a weight loss of *ca* 10.12% (calcd 10.14%) corresponding to the loss of C_3NH_5 organic moiety. The last step is due to the loss of C_7H_4 organic molecule with a weight loss of *ca* 16.21% (calcd 16.23%) leaving lanthanum oxide contaminated with carbon as a residue. The total weight loss amounts to 60.52% (calcd 61.12%).

TGA data of **2** were recorded in the temperature range from 10 to 1000 °C. The thermogram of the complex shows three stages of weight loss. The complex shows an initial weight loss at 30–150 °C which corresponds to the loss of three water molecules, HCl and H_2 molecules, and is accompanied by a weight loss of *ca* 16.02% (calcd 16.12%). The second step of decomposition occurred at 150–415 °C corresponding to the loss of $C_4N_2H_4$ organic molecule, and is accompanied by a weight loss of *ca* 13.97% (calcd 14.02%). The complex showed a weight loss around 415–1000 °C of *ca* 13.12% (calcd 13.14%) corresponding to continuous sublimation of organic ligand moieties $½C_2H_2O$ and C_4H_6 and the formation of an air-stable metal oxide contaminated with carbon as the end product. The results agreed well with the composition of the metal complex. The total weight loss amounts to *ca* 43.11% (calcd 43.28%).

The TGA curve of **3** shows three stages of decomposition. The first step occurs in the range 30–100 °C with a weight loss of *ca* 14.47% (calcd 14.48%) corresponding to the elimination of $2.5H_2O$, HCl and H_2 molecules. The second step, which occurs in the range 100–340 °C, is assigned to the loss of part of the ligand in the complex $C_4H_{10}N_2O$ (observed weight loss of *ca* 17.64%; calcd 17.69%). The third step, which occurs in the range 340–1000 °C, is assigned to the loss of $C_{10}H_2$ organic part (observed weight loss of *ca* 20.98%; calcd 21.16%). Finally, the stable metal oxide was formed contaminated with carbon as a residue. The total weight loss amounted to *ca* 53.09% (calcd 53.33%).

3.5 | Structural interpretation

The structures of the complexes of H_2L with La(III), Er(III) and Yb(III) ions were confirmed from the elemental analyses, FT-IR, ^1H NMR, molar conductance, UV–visible and TGA data. The elemental and spectral analyses revealed that the complexes were of the type $[M(L)(H_2O)_2]Cl{\cdot}H_2O$, (M = La(III), Er(III), Yb(III)). The FT-IR spectral data suggest that the ligand coordinated in a tetradentate manner (ONNO) via two deprotonated phenolic oxygen atoms and two nitrogen atoms of azomethine (C=N) groups. Conductance measurements confirmed the complexes as 1:1 electrolytes. On the basis of the above observations, an octahedral geometry is suggested for the investigated complexes. The structures of the complexes are shown in Figure 5.

3.6 | Biological activity study

The principal aim of any antimicrobial compound is to inhibit microbial activity without any side effects to patients.[43] The biological activity of Schiff bases is known and it is mainly attributed to the azomethine group.[44] Overall, this activity is enhanced by complexing with a metal, but it is also influenced by its nature and coordination mode. The biological activity of the metal complexes depends on the following factors:

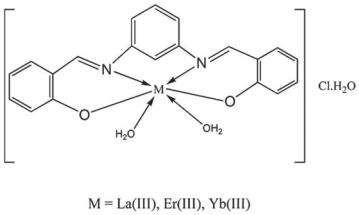

FIGURE 5 Structures of metal complexes of the Schiff base ligand (H_2L)

i. The chelate effect of the ligands.
ii. The total charge on the complex ion.
iii. The nature of the donor atoms.
iv. The nature of the counter ions that neutralize the complex.
v. The nature of the metal ion.
vi. The geometrical structure of the complex.

The increased activity of the metal chelates can be explained on the basis of chelation theory.[43–45] According to the concept of cell permeability, the lipid membrane surrounding a cell favours the passage of only lipid-soluble materials due to the fact that liposolubility is considered to be an important factor that controls antimicrobial activity. On chelation, the polarity of the metal ion will be reduced to a greater extent due to the partial sharing of positive charge of metal ions with donor groups and the overlap of the ligand orbital. Furthermore, it increases the delocalization of the electrons over the whole chelate ring and enhances the lipophilicity of the complex. This increased lipophilicity enhances the penetration of the complexes into the lipid membrane which can then block the metal binding sites on enzymes of microorganisms. These metal complexes also disturb the respiration process of the cell and thus block the synthesis of proteins, which restricts further growth of the organism. The variation in the activity of different complexes against different organisms depends either on the impermeability of microbe cells or difference in microbe ribosomes.

The prepared complexes involve three different metals, lanthanum, erbium and ytterbium, having N_2O_2 coordination. The ligand and its complexes were screened for antimicrobial activity in DMSO solvent as a control substance. The compounds were tested with the same concentrations in DMSO solution (0.25 $\mu g\ \mu l^{-1}$). Furthermore, the antibacterial activity of these compounds was also compared with that of commercial antibiotics, namely ampicillin and gentamycin, and the antifungal activity was compared with that of amphotericin B. All the synthesized compounds exhibited varying degrees of inhibitory effects on the growth of different test strains. In general, the metal complexes are more potent bactericides than the ligand. The antibacterial screening results exhibited marked enhancement in activity on coordination with the metal ions against test bacterial strains. It has also been suggested[46] that ligands with nitrogen and oxygen donor systems might inhibit enzyme production, since the enzymes which require these groups for their activity appear to be especially susceptible to deactivation by the metal ions upon chelation. So the enhanced activities of the metal complexes compared to the free ligand may

TABLE 4 Biological activity of H_2L and its metal complexes[a]

Sample	Inhibition zone diameter (mm mg^{-1} sample)						
	S. aureus (G^+)	*B. subtilis* (G^+)	*Salmonella* sp. (G^-)	*E. coli* (G^-)	*P. aeruginosa* (G^-)	*A. fumigatus*	*C. albicans*
Control: DMSO	0	0	0	0	0	0	0
H_2L	10	14	12	13	17	15	17
1	13	16	20	13	13	28	27
2	14	17	19	14	14	24	20
3	14	18	21	15	15	26	29
Ampicillin	23	32	—	—	—	—	—
Gentamycin	—	—	17	19	16	—	—
Amphotericin B	—	—	—	—	—	23	25

[a]Numbers are given in section 2.

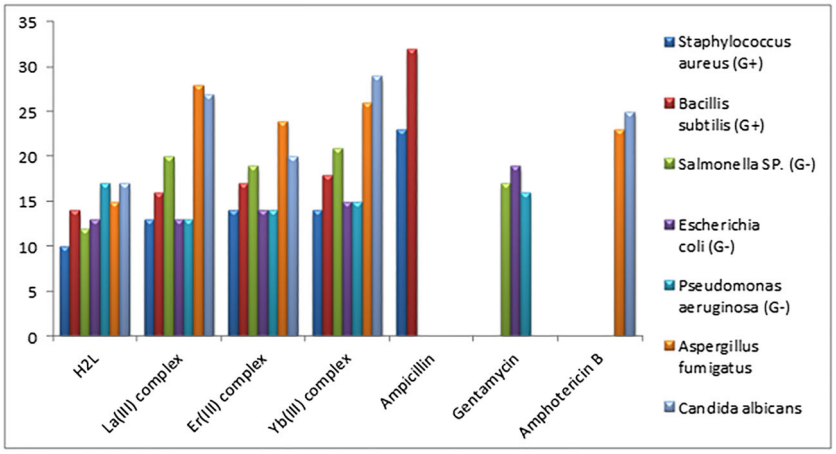

FIGURE 6 Biological activity of the Schiff base ligand (H_2L) and its metal complexes

be attributed to the increase in the number of oxygen groups around the central metal atom arising from chelation, and hence the central metal atom was not only responsible for biological activity because some metal complexes can enhance activity and others can reduce activity with respect to the parent ligand.[47] The orbital of each metal ion is made so as to overlap with the ligand orbital. Increased activity enhances the lipophilicity of complexes due to delocalization of π-electrons in the chelate ring.[48] In some cases increased lipophilicity leads to breakdown of the permeability barrier of the cell.[43,49,50] The antibacterial activity of H_2L and its metal(III) complexes were studied against three Gram-negative and two Gram-positive bacterial strains according to the literature protocol. The results are summarized in Table 4 and shown in Figure 6. The obtained results were compared with those for standard drugs ampicillin and gentamycin. The antifungal activity was studied against *C. albicans* and *A. fumigates*. It was observed that the complexes have higher antibacterial activity than the ligand against *S. aureus*, *B. subtilis*, *Salmonella* sp. and *E. coli*. Against *C. albicans* and *A. fumigates* fungi, the biological activity of the metal complexes was found to be higher than that of the free ligand.

4 | CONCLUSIONS

The newly synthesized ligand H_2L derived from *m*-phenylenediamine with 2-hydroxybenzaldehyde (1:2) after reaction with respective metal salts yielded metal complexes of the type $[ML(H_2O)_2]\cdot H_2O\cdot Cl$ (M = La(III), Er(III), Yb(III)) having an octahedral geometry around the metal ions. The ligand and its complexes were characterized using elemental analyses, FT-IR, ^1H NMR and UV–visible spectra, molar conductance measurements and TGA. The FT-IR spectral data of the prepared complexes indicate that the ligand behaves as a binegative tetradentate ligand through ONNO coordination sites and coordinated to the metal ions via the deprotonated phenolic oxygen and azomethine nitrogen atoms with 1:1 (metal-to-ligand) stoichiometry for all complexes.

Spectral studies and molar conductivity measurements of the metal complexes were used to determine the type of coordination and the geometry around the central metal ion. The conductance data revealed that all complexes were 1:1 electrolytes in DMF. TGA studies of the complexes also helped to characterize the complexes. All complexes were found to have coordinated water molecules and water of crystallization. Further studies were carried out for their antibacterial activities, revealing that the metal complexes are more effective in their antibacterial activities than the free ligand.

ORCID

M.A. Diab https://orcid.org/0000-0002-9042-1356
Gehad G. Mohamed https://orcid.org/0000-0002-1525-5271
W.H. Mahmoud https://orcid.org/0000-0001-9187-4325
A.Z. El-Sonbati https://orcid.org/0000-0001-7059-966X
Sh.M. Morgan https://orcid.org/0000-0002-8921-4894

REFERENCES

[1] A. D. Garnovskii, I. G. Vasil'chenko, *Usp. Khim.* **2005**, *74*, 211.

[2] W. H. Mahmoud, G. G. Mohamed, O. Y. El-Sayed, *Appl. Organometal. Chem.* **2018**, *32*, e4051.

[3] G. Newkome, J. D. Sauer, J. M. Roper, D. C. Hager, *Chem. Rev.* **1977**, *13*, 513.

[4] G. G. Mohamed, W. H. Mahmoud, M. A. Diab, A. Z. El-Sonbati, S. Y. Abbas, *J. Mol. Struct.* **2019**, *1181*, 645.

[5] E. E. Lambert, B. Chabut, S. Chardon-Noblat, A. Deronzier, G. Chottard, A. Bousseksou, J. P. Tuchagues, J. Laugier, M. Bardet, J.-M. Latour, *J. Am. Chem. Soc.* **1997**, *199*, 9424.

[6] D. E. Fenton, *Inorg. Chem. Commun.* **2002**, *5*, 537.

[7] N. N. Murthy, M. Mahroof-Taher, K. D. Harlin, *Inorg. Chem.* **2001**, *40*, 628.

[8] P. P. Gamez, J. von Harras, O. Roubeau, W. L. Driessen, J. Reedijk, *Inorg. Chim. Acta* **2001**, *324*, 27.

[9] Sh. M. Morgan, A. Z. El-Sonbati, H. R. Eissa, *J. Mol. Liq.* **2017**, *240*, 752.

[10] Z. Kazemi, H. A. Rudbari, V. Mirkhani, M. Sahihi, M. Moghadam, S. Tangestaninejad, I. Mohammadpoor-Baltork, *J. Mol. Struct.* **2015**, *1096*, 110.

[11] A. Z. El-Sonbati, M. A. Diab, A. M. Eldesoky, Sh. M. Morgan, O. L. Salem, *Appl. Organometal. Chem.* **2019**, *33*, e4839.

[12] M. S. Nair, D. Arish, R. S. Joseyphus, *J. Saudi Chem. Soc.* **2012**, *16*, 83.

[13] L. H. Abdel-Rahman, R. M. El-Khatib, L. A. E. Nassr, A. M. Abu Dief, M. Ismail, A. A. Seleem, *Spectrochim. Acta* **2014**, *117*, 336.

[14] L. N. Ji, X. H. Zou, J. G. Liu, *Coord. Chem. Rev.* **2001**, *216*, 513.

[15] Sh. M. Morgan, A. Z. El-Sonbati, M. A. El-Mogazy, *Appl. Organometal. Chem.* **2018**, *32*, e4264.

[16] A. Z. El-Sonbati, M. A. Diab, Sh. M. Morgan, A. M. Eldesoky, M. Z. Balboula, *Appl. Organometal. Chem.* **2018**, *32*, e4207.

[17] A. Z. El-Sonbati, M. A. Diab, Sh. M. Morgan, H. A. Seyam, *J. Mol. Struct.* **2018**, *1154*, 354.

[18] A. Z. El-Sonbati, M. A. Diab, Sh. M. Morgan, M. A. El-Mogazy, *Appl. Organometal. Chem.* **2018**, *32*, e4530.

[19] a) A. Z. El-Sonbati, M. A. Diab, Sh. M. Morgan, M. Z. Balboula, *Appl. Organometal. Chem.* **2018**, *32*, e4059. b) Sh. M. Morgan, M. A. Diab, A. Z. El-Sonbati, *Appl. Organometal. Chem.* **2018**, *32*, e4281.

[20] W. H. Mahmoud, R. G. Deghadi, G. G. Mohamed, *Appl. Organometal. Chem.* **2018**, *32*, e4289.

[21] M. A. Pfaller, L. Burmeister, M. A. Bartlett, M. G. Rinaldi, *J. Clin. Microbiol.* **1988**, *26*, 1437.

[22] National Committee for Clinical Laboratory Standards. Reference method for broth dilution antifungal susceptibility testing of conidium-forming filamentous: proposed standard M38-A. Wayne, PA, **2002**.

[23] National Committee for Clinical Laboratory Standards. Method for antifungal disc diffusion susceptibility testing of yeast: proposed guideline M44-P, Wayne, PA, **2003**.

[24] L. D. Liebowitz, H. R. Ashbee, E. G. V. Evans, Y. Chong, N. Mallatova, M. Zaidi, D. Gibbs, *Diagn. Microbiol. Infect. Dis.* **2001**, *4*, 27.

[25] M. J. Matar, L. O. Zeichner, V. L. Paetznick, J. R. Rodriguez, E. Chen, J. H. Rex, *Agents Chemother.* **2003**, *47*, 1647.

[26] K. K. Abid, A. B. Omar, *Res. Chem. Intermed.* **2015**, *41*, 1715.

[27] R. Anbazhagan, K. R. Sankaran, *J. Mol. Struct.* **2013**, *1050*, 73.

[28] O. A. El-Gammal, G. M. Abu El-Reash, S. E. Ghazy, A. H. Radwan, *J. Mol. Struct.* **2012**, *1020*, 6.

[29] A. S. Munde, A. N. Jagdale, S. M. Jadhav, T. K. Chondhekar, *J. Serb. Chem. Soc.* **2010**, *75*, 349.

[30] Sh. M. Morgan, M. A. Diab, A. Z. El-Sonbati, *Appl. Organometal. Chem.* **2018**, *32*, e4305.

[31] Sh. M. Morgan, M. A. Diab, A. Z. El-Sonbati, *Appl. Organometal. Chem.* **2018**, *32*, e4504.

[32] G. G. Mohamed, A. A. El-Sherif, M. A. Saad, S. E. A. El-Sawy, Sh. M. Morgan, *J. Mol. Liq.* **2016**, *223*, 1311.

[33] M. A. Diab, A. Z. El-Sonbati, Sh. M. Morgan, M. A. El-Mogazy, *Appl. Organometal. Chem.* **2018**, *32*, e4378.

[34] A. Z. El-Sonbati, M. A. Diab, Sh. M. Morgan, *J. Mol. Liq.* **2017**, *225*, 195.

[35] H. M. Refaat, H. A. El-Badway, Sh. M. Morgan, *J. Mol. Liq.* **2016**, *220*, 802.

[36] A. Z. El-Sonbati, A. A. M. Belal, M. S. El-Gharib, Sh. M. Morgan, *Spectrochim. Acta A* **2012**, *95*, 627.

[37] A. Z. El-Sonbati, M. A. Diab, A. A. M. Belal, Sh. M. Morgan, *Spectrochim. Acta A* **2012**, *99*, 353.

[38] M. I. Abou-Dobara, A. Z. El-Sonbati, Sh. M. Morgan, *World J. Microbiol. Biotechnol.* **2013**, *29*, 119.

[39] N. A. El-Ghamaz, A. Z. El-Sonbati, Sh. M. Morgan, *J. Mol. Struct.* **2012**, *1027*, 92.

[40] G. G. Mohamed, H. F. Abd El-Halim, M. M. I. El-Dessouky, W. H. Mahmoud, *J. Mol. Struct.* **2011**, *111*, 29.

[41] H. F. Abd El-Halim, G. G. Mohamed, M. M. I. El-Dessouky, W. H. Mahmoud, *J. Pharm. Res.* **2012**, *5*, 5084.

[42] W. H. Mahmoud, G. G. Mohamed, N. F. Mahmoud, *Appl. Organometal. Chem.* **2017**, *31*, e3583.

[43] H. F. Abd El-halim, M. M. Omar, G. G. Mohamed, *Spectrochim. Acta A* **2011**, *78*, 36.

[44] M. X. Li, L. Z. Zhang, C. L. Chen, J. Y. Niu, B. S. Ji, *J. Inorg. Biochem.* **2012**, *106*, 117.

[45] M. I. Abou-Dobara, N. F. Omar, M. A. Diab, A. Z. El-Sonbati, Sh. M. Morgan, M. A. El-Mogazy, *J. Cell. Biochem.* **2019**, *120*, 1667.

[46] P. G. Avajia, C. H. V. Kumarb, S. A. Patilc, K. N. Shivanandad, C. Nagaraju, *Eur. J. Med. Chem.* **2009**, *44*, 3552.

[47] H. F. A. El-Halim, G. G. Mohamed, M. M. I. El-Dessouky, W. H. Mahmoud, *Spectrochim. Acta A* **2011**, *82*, 8.

[48] H. W. Horowitz, G. M. Jetzger, *Anal. Chem.* **1963**, *35*, 1464.

[49] G. G. Mohamed, M. H. Soliman, *Spectrochim. Acta A* **2010**, *76*, 341.

[50] A. N. M. A. Alaghaz, R. A. Ammar, *Eur. J. Med. Chem.* **2010**, *45*, 1314.

How to cite this article: Diab MA, Mohamed GG, Mahmoud WH, El-Sonbati AZ, Morgan SM, Abbas SY. Inner metal complexes of tetradentate Schiff base: Synthesis, characterization, biological activity and molecular docking studies. *Appl Organometal Chem*. 2019;e4945. https://doi.org/10.1002/aoc.4945